An Enhanced Two-Dimensional Hole Gas (2DHG) C-H Diamond with Positive Surface Charge Model for Advanced Normally-Off MOSFET Devices

Reem Alhasani
Waseda University
Taichi Yabe
Waseda University
Yutaro Iyama
Waseda University
Nobutaka Oi
Waseda University
Shoichiro Imanishi
Waseda University
Quang Nguyen
Waseda University
Hiroshi Kawarada (kawarada@waseda.jp)
Waseda University

Research Article

Keywords: MOSFETs, FETs, 2D, DC

Posted Date: December 29th, 2020

DOI: https://doi.org/10.21203/rs.3.rs-128027/v1

Version of Record: A version of this preprint was published at Scientific Reports on March 10th, 2022. See the published version at https://doi.org/10.1038/s41598-022-05180-4.

An Enhanced Two-Dimensional Hole Gas (2DHG) C-H Diamond with Positive Surface Charge Model for Advanced Normally-Off MOSFET Devices

Reem Alhasani[1,5], Taichi Yabe[1], Yutaro Iyama[1], Nobutaka Oi[1], Shoichiro Imanishi[1], Quang Ngoc Nguyen[4], Hiroshi Kawarada[1,2,3] *

[1]Department of Nano Science and Nano Engineering, School of Advanced Science and Engineering, Waseda University, Shinjuku, Tokyo 169-8555, Japan.
[2]Kagami Memorial Research Institute for Materials Science and Technology, Waseda University, 2-8-26 Nishiwaseda, Shinjuku, 169-0051 Tokyo, Japan.
[3]Research organization for Nano and Life Innovation, Waseda University, 513 Waseda-Tsurumaki, Shinjuku, Tokyo 169-0041, Japan.
[4]Department of Communications and Computer Engineering, School of Fundamental Science and Engineering, Waseda University, Shinjuku, Tokyo 169-0051, Japan.
[5]National Center of Nano and Semiconductor, King Abdulaziz City for Science and Technology, 12354 Riyadh, Saudi Arabia.
*** Correspondence should be addressed to Hiroshi Kawarada (kawarada@waseda.jp)**

Though the complementary power field effect transistors (FETs), e.g., metal-oxide-semiconductor-FETs (MOSFETs) based on wide bandgap materials, enable low switching losses and on-resistance, p-channel FETs are not feasible in any wide bandgap material other than diamond. In this paper, we propose the first work to investigate the impact of fixed positive surface charge density on achieving normally-off and control threshold voltage operation obtained on p-channel two-dimensional hole gas (2DHG) hydrogen-terminated diamond (C-H) FET using deep nitrogen doping in the diamond substrate. In general, a p-channel diamond C-H MOSFET demonstrates normally-on operation, but the normally-off operation is also a critical requirement of the feasible electronic power devices in terms of safety operation. The evaluation results of the characteristic of the C-H MOSFET capacitor with the two demonstrated charge sheet models using the two-dimensional Silvaco Atlas TCAD show that the fixed-Fermi level is a function of capacitance-voltage with an activation energy of 1.7 eV (donor level) at the H-diamond surface close to the minimum conduction band. The maximum current density with a positive surface charge model and a nitrogen-doped layer of the Al_2O_3/H-diamond device is -52 mA/mm at a gate-source voltage of -42 V. Also, the gate threshold voltage is relatively high at V_{th}= -3 V, i.e., the positive surface charge model can achieve the normally-off operation. Moreover, we demonstrate that the obtained results correspond to the experimental work with the SiO_2 layer located below the gate in C-H diamond/Al_2O_3 surface.

Diamond is the most valuable material, which is widely used in electronic device applications, thanks to its distinctive properties compared with other semiconductor materials, e.g., silicon carbide (SiC), germanium (Ge), and gallium nitride (GaN). Typically, the electric property of diamond enables the wide bandgap of the diamond at 5.45eV which enhances the device toughness with a high carrier's mobility at 4500 cm^2/Vs and 3800 cm^2/V.s for electron and hole, respectively[1], and a high thermal conductivity at 22 W/cm.k as well[2]. These unique matching properties of the diamond make it a promising material to be used as the substrate of electronic devices, and also the surface of the FET electronic device is a significant region due to its direct impact on the DC operation of the device. For example, hydrogen terminated-

diamond surfaces were explained in terms of surface reconstruction and surface type conduction, then demonstrated to be suitable for electron device application with surface stability[3]. In the case of metal–oxide–semiconductor FETs (MOSFETs), the hydrogen termination can effectively induce the conductivity channel with the interface charge (fixed surface charge) in the electronic device surface. This characteristic makes hydrogen-terminated (C-H) diamond with p-channel conduction an emerging research topic, which develops feasible high power/high-frequency devices such as high-power FET for different applications, e.g., the inverter systems[4]. This positive hydrogenated charge facilitates the adsorption process of the negative surface fixed charge, which is induced at the diamond surface from atmospheric[5]. Hence, the two-dimensional hole gas (2DHG) layer is located nearby the interface with a high hole carrier's density around 10^{13}cm^{-2} (10^{20} cm^{-3})[6,7,8]. In contrast, the surface of the diamond is insulated from oxygen termination led to disappearing surface conduction. When the crystal structure of the atoms is terminated, an unsatisfied bond, called "dangling bond" will be left, the surface energy will be increased[9]. As the high surface energy is not desired, this surface energy should be decreased in terms of the number of dangling bonds leading to atoms so that they can reach a new position with satisfied bonds at the surface. Also, the negative electron affinity of the diamond at -1.3 eV occurs after H-termination depending on C-H dipoles[10]. This distinguished property has a strong relationship with a chemisorbed species on the H-terminated diamond surface[11]. Up to now, our research team has successfully reproduced the FETs characteristic of C-H diamond FET using the 2-dimensional (2D) negative charge sheet model[1] and the 2D acceptor model[12]. Typically, these acceptors or negatively charged sites scatter the centers for carrier (holes) transport near the C-H surface[4]. Also, the 2DHG layer can be obtained on the C-H diamond surface using acceptor or negative surface charge to establish the depletion mode, called normally-on. The C-H diamond MOSFET device usually has a normally-on operation in this context, as identified in our prior work[13]. However, the normally-off operation is required for the electronic power device to confirm the electric system protection from the perspective of safety and device feasibility. Kitabayashi et al.[14] achieved a normally-off operation of the C-H diamond MOSFET undoped layer with a partially oxidized channel under the gate. Also, the device exhibits satisfied normally-off operation with distinguished characteristics depending on nitrogen concentration using the ion implantation process[15]. Saito et al.[16] achieved the normally-off operation of high-voltage AlGaN/GaN high-electron mobility transistors (HEMTs) for power electronic applications to reduce 2DEG density. In addition, Liu et al.[17] confirmed the normally-off device operation using HfO_2-gate MOSFETs. Fei et al.[18] fabricated the two kinds of diamond metal oxide semiconductor field effect transistors (MOSFETs) electronic device, with a C–Si diamond channel (SiO_2). In the study, there are undoped and heavily boron-doped in contact area (source/drain), and both of the MOSFET devices exhibited normally-off FET characteristics (enhancement mode). However, there has not been any reported result on a positive surface charge model in the normally-off achieved in the FET device. Thus, in this research, we demonstrate the first study on the normally-off operation (enhancement mode) using a positive surface charge model of 2DHG Ib (001) Diamond MOSFETs, with full deep Nitrogen doping layer in diamond, where N is 1.7 eV donor in the diamond. Toward this end, to achieve the enhancement mode, i.e., normally-off, we simulated the positive surface charge sheet model with deep donor using a Nitrogen-doped layer in an intrinsic diamond substrate. We investigated this model for controlling threshold voltage value to achieve normally-off. The gate threshold voltage without applying surface charge is minimal (almost zero), indicated that the device is in a natural state. Also, we take the fixed positive charge as low as possible (5×10^{11} cm^{-2}) and using Nitrogen (donor) in the concentration of 1×10^{16} cm^{-3} and boron-doped diamond substrate in the concentration of 4×10^{15}cm^{-3}. Typically, the nitrogen should be used with boron in the same place because the diamond cannot be fully ionized by nitrogen only[19]. However, in this research

work, normally-off of hydrogen-terminated diamond (C-H) diamond MOSFET is performed and achieved with substrate doping using a nitrogen-doped layer with an activation energy of 1.7 eV with positive surface charge since we could not achieve the normally-off state without applying the surface charge as the device is in a neutral state with substrate doping, as aforementioned. We use the diamond substrate doping by nitrogen (donor) to successfully achieve the normally-off state with a positive fixed surface charge of the MOSFET device. This technique is used to achieve a higher level of the negative value of the gate threshold voltage (V_{th}), where the maximum current density cannot be obtained without diamond doping using a positive surface charge in the 2DHG MOSFET device. The research also demonstrates that the proposal is a highly potential method to achieve the normally-off operation (enhancement mode) in the diamond MOSFET devices under specific conditions, e.g., nitrogen-doped in the bulk conduction.

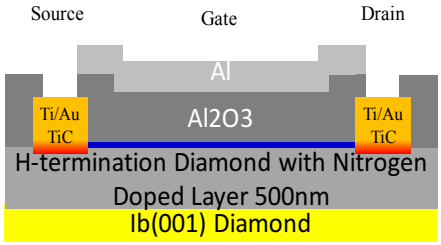

Figure 1. Cross-sectional representation of the 2DHG diamond MOSFET with deep donor nitrogen doping (500 nm) where L_G = 22 µm, L_{ch} =21 µm and W_G = 25 µm.

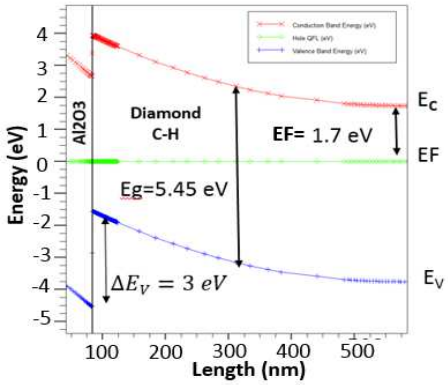

Figure 2. Schematic energy diagrams of the 2DHG diamond MOSFET device. The band of hydrogynated diamond become upward in the positive surface charge model with N deep doping (1.7 eV) at the inversion layer.

Results

The deep nitrogen doping with activation energy at 1.7 eV in low concentration in the diamond substrate (bulk) is a requirement to build the structure of MOSFET device with p-channel C-H Hydrogenated-diamond using positive fixed surface charge to achieve the normally-off device operation. The DC operation of 2DHG hydrogenated diamond MOSFET device simulation is carried out via various surface charge sheet models. The normally-on operation is performed by the negative surface charge sheet model, whereas the positive surface charge sheet model with deep donor doping is dedicated to achieving the normally-off operation. Also, the third model is a non-surface charge sheet model that gives flat band condition and possibility of control hole mobility due to no ion scattering, given that the ion scattering is described as a Coulomb interaction of the two particles. We considered the MOSFET C-H diamond, as depicted in Fig. 1, with a gate length of L_G= 22µm, a gate width of W_G= 25µm, a passivation oxide ALD-Al_2O_3 with a thickness of t_{ox}= 100 nm, a source-drain length of L_{SD}= 21µm, and a C-H diamond substrate with a thickness of 500 nm and the doping thickness of 500 nm.

Next, we calculate the Fermi level position of the MOSFET hydrogenated-diamond device with a low boron concentration of 4×10^{15} cm^{-3} and donor doping with a low nitrogen concentration of 1×10^{16} cm^{-3} in the freeze-out region. This approach corresponds to the research work conducted by Collins et al.[19], which showed that the donor in diamond is different from other materials, e.g., silicon or germanium, then makes the nitrogen doping in diamond hard to be ionized since nitrogen is a noble gas. The authors then considered that the

Fermi level could be clearly pinned nearby the conduction band by the effect of nitrogen doping (10^{17} cm^{-3}) with boron doping (10^{16} cm^{-3}) in the same position. We apply the formula to calculate the Fermi position of carriers in the freeze-out region[19] as follows:

$$E_F = (E_g - E_D) + K_\beta T \, ln\left(\frac{N_d - N_a}{2N_a}\right) \qquad for\ N_d > N_a \tag{1}$$

where E_g is a bandgap, E_D is a donor ionization energy (activation energy), K_β is the Boltzmann constant, T is a temperature, N_d and N_a are the donor and acceptor concentration, respectively.

An interesting obtained result of the Fermi level position in the p-channel is that it is close to the interface of diamond with deep nitrogen doping (donor) pinning at about 1.7eV (acceleration energy) under the conduction band minimum. The reason behind Fermi level pinning in this position is that the charge traps use deep donor, then leading to shifting the Fermi level close to the conduction band at the surface as we found out in literature[20]. Specifically, the band diagram in the C-H diamond surface moves upward with the band binding, and the valence band maximum crosses the Fermi level, i.e., high hole accumulation under valence band maximum when applying the high negative gate bias in the negative charge sheet model. From our prior study, we observed that p-channel with positive hole carriers is a type of MOSFET device after hydrogen is terminated from diamond[7], and the 2DHG layer is confirmed when the fixed surface charge is applied in the hydrogenated-diamond surface. Specifically, the inversion layer is observed when applying the negative gate voltage so that the occupied electron acts as a negative charge in the passivation oxide layer Al_2O_3 (as the Atomic Layer Deposition (ALD) of 2DHG on a C-H diamond surface), then attracts the unoccupied hole flow in the channel to interface between the oxide and substrate, and usually leads to the formation of conducting layer as a channel[1].

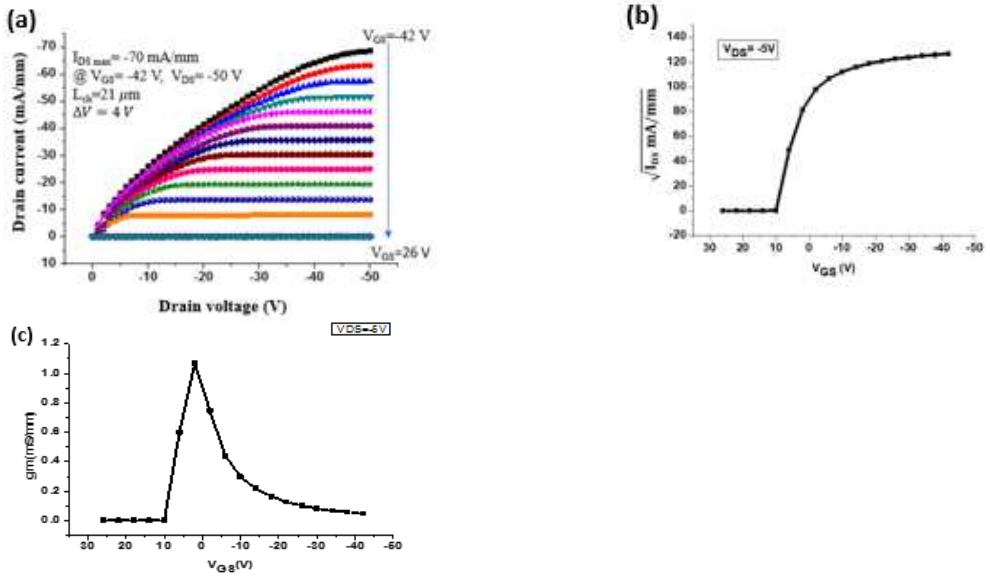

Figure 3. Schematic diagram of characteristics of 2DHG diamond MOSFET in a negative surface charge model. Applied Qf= -5x10^{12} cm^{-2} with N doping layer. **(a)** The $I_{DS\ Max}$= -70 mA/mm at V_{DS} is in the range of 50 V, and V_G ranges from 26V to -42 V with a voltage step of 4 V. **(b)** Threshold voltage V_{th} = 10 V indicating the normally-on state at V_{DS} = -5 V. **(c)** Transconductance of device gm= 1.1 mS/mm.

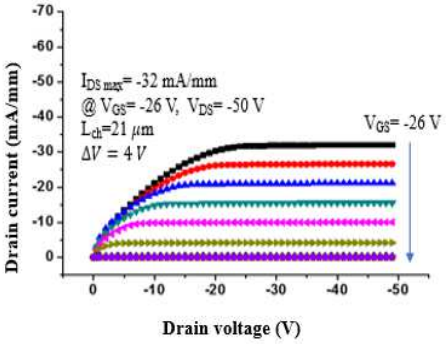

Figure 4. Schematic diagram of I_{DS}–V_{DS} characteristics of 2DHG diamond MOSFET in the natural surface charge model (non-charged) with N doping layer. Applied V_{DS} is in the range of 50V, and V_G ranges from 26 V to -26 V with a voltage step of 4 V.

In addition, the ionization of the donor or the acceptor is based on the position of the impurity level, which is close to the conduction band or valence band, i.e., depending on the concentration value of the carrier's impurities. Thus, we evaluate the proposal by using a low concentration of boron in activation energy 0.37 eV with deep doping of nitrogen at room temperature of 300° C in the same position as of full C-H diamond at 500 nm to create a full ionization state and ensure that the Fermi position is pinned in the same position of the donor level, which is 1.7 eV[19]. In the bandgap of a diamond, the nitrogen is occupied by an electron that is joined with carbon (diamond) bonds dangling and π bonds. Then the unoccupied state can be observed near the Fermi level, which can push electrons towards the minimum conduction band[21]. Hence, the conductivity is obtained by the newly occupying state of carbon in the bandgap, and the Fermi level is very close to the conduction band, i.e., a high transporting electron leads to a high electrical conductivity in the grains boundary (GB) diamond film[22].

We then compare two models of fixed surface charge, negative and positive surface charge sheet models, within deep nitrogen doping in full C-H hydrogen-terminated diamond. In the negative surface charge model, the C-H surface adsorption is very high because the negative ions in the insulator layer Al_2O_3 are regarded as negative charge and attracted to the surface. Then, the dipole bond is created within the positive ions, which are from hydrogen termination in the diamond and the Fermi level located close to the conduction band due to nitrogen doping. However, in the positive surface charge model, which leads to the enhancement mode (normally-off), the Fermi level position is pinned close to the conduction band at 1.7 eV. The band diagram also turns upward in this case due to nitrogen doping with a positive charge that applies close to the surface. The hydrogen-terminated diamond and the negative charge of Al_2O_3 have induced the 2DHG layer. The valence band, however, does not cross the Fermi level because the MOSFET hydrogen-terminated diamond is normally-off (enhancement mode). The reason is that the positive charge prevents the C-H surface from causing positive ions pinned in the channel. Hence, the adsorption in the C-H surface becomes very weak, which leads to the normally-off state as clarified in our recent work[5].

Also, Fig. 2 shows the band bending diagram with a changed Fermi level in the same position at the activation energy of nitrogen after applying the positive fixed surface charge sheet model, which is usually pinned in the mid-bandgap of the diamond. From the simulation result, we found out that the ideal Schottky contact of SBH between the drain contact (Au/Ti) and the hydrogenated-diamond surface of the MOSFET C-H device is 0.19 eV (~0.2 eV) which indicates the status of the Ohmic contacts. In contrast, the large value of SBH cannot obtain that state[23]. Ohmic properties were obtained when metals with higher electronegativity, such as Pt, Au, Pd, and Ag, were used. In those cases, the SBHs of the diodes were assumed to be less than 0.3 eV[3]. Also, TiC was effective in formatting the Ohmic contact. The valence band offset (ΔE_V) between the edge of the valence band in C-H diamond and passivation layer Al_2O_3 is in the range of 3~4 eV.

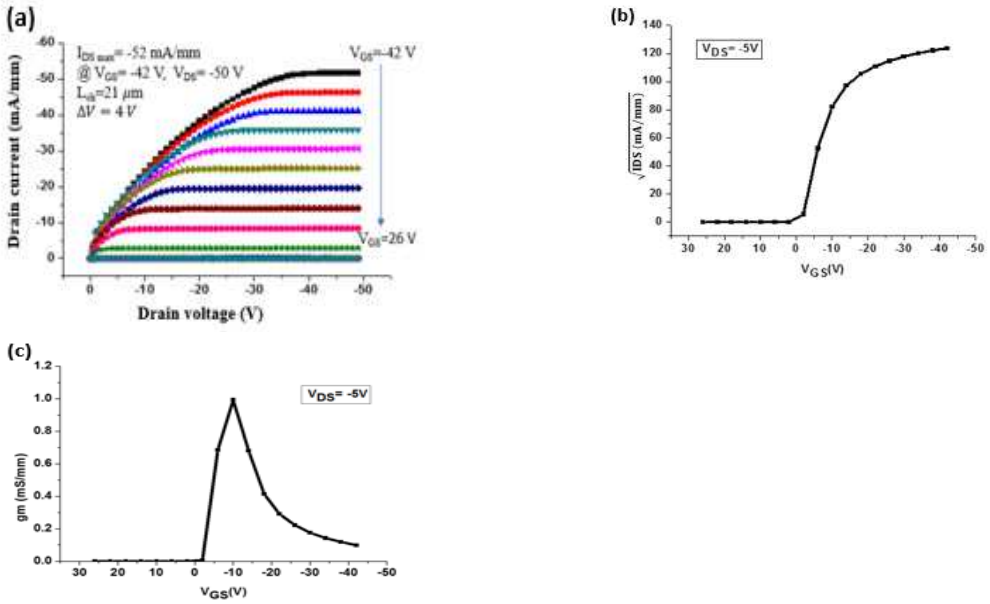

Figure 5. Schematic diagram of output characteristics of 2DHG diamond MOSFET positive surface charge model of $5x10^{11}cm^{-2}$ with nitrogen doping layer in concentration at $1x10^{16}cm^{-3}$ at room temperature. **(a)** I_{DS}-V_{DS} characteristics, the $I_{DS\ Max}$= -52 mA/mm at V_{DS} is in the range of 50 V, and V_G ranges from 26V to -42 V with a voltage step of 4 V **(b)** Threshold voltage V_{th} = -3V at drain voltage V_{DS} = -5 V indicating the normally-off state. **(c)** Transconductance of device gm = 1.0 mS/mm.

As can be observed from the I_{DS}-V_{DS} characteristic in Fig.3 (a), the drain current density I_{DS} of the hydrogenated-diamond MOSFET with the negative surface charge model ($-5x10^{12}cm^{-3}$) exceeds -70 mA/mm at a drain bias of -50 V. The evaluation result also shows the saturation behavior in the Ohmic region when the gate bias is greater than 0V, and the pinch-off is observed when V_{GS} is 26V. The drain current gets more linear behavior when we apply a more negative value than -42 V for gate bias. Fig. 3 (a) shows that the threshold voltage V_{th} is 10V at drain voltage -5V, which indicates the normally-on operation. In addition, Fig. 3(c) shows that the transconductance of the device is a constant of 1.1mS/mm when the drain current V_{DS} at -5V for all types of models. In the non-charge model, the I_{DS}-V_{DS} characteristic plot depicts the saturation behavior when the maximum drain current density is 32mA/mm, and the threshold voltage is already zero. Moreover, Fig. 4 shows the device characteristics I_{DS}-V_{DS} and V_{th}, respectively. In this case, no ion scattering in the interface leads to the possibility of a controlling carrier's mobility. When hole mobility is increased in the device, we observe a sharp increase in drain current density saturation. In this context, the MOSFET C-H diamond device with a positive surface charge demonstrates the performance goal. The significant increase in I_{DS} is apparently compared to the case of partial nitrogen ion implantation MOSFET device when L_G and L_{SD} have the same values in the same condition[14]. However, the drain current is still located in the saturation region, even when we increase the gate voltage to a very high value. Thus, we need to suppress the variation of the drain current with the gate voltage by controlling gate resistance and increasing the drain current for the MOSFET power device.

We then measure the DC operation (I_{DS}-V_{DS} characteristic) of the MOSFET device by identifying the impact of drain-source current I_{DS} on the drain-source voltage in the linear scale of the positive fixed surface charge model. The operation is completely pinch-off at a gate bias of 26V and saturated in the Ohmic region when the applied negative gate bias is -42V, and the drain voltage is -50V, with a voltage step of 4V. This result shows that we can achieve high current density as a function of the drain voltage of the MOSFET 2DHG hydrogenated-diamond device with nitrogen-doped bulk when the gate bias is negative, i.e., $V_{GS} < 0$. Specifically, Fig. 5(a) illustrates the I_{DS}-V_{DS} characteristic with the positive fixed surface charge,

in which maximum current density is $I_{DS\ Max}$ = -52 mA/mm when the channel length (distance between the source and drain) is 21µm and overlapping gate length is 22µm. The drain current behavior is saturated when we increase the highest gate bias to -42V. The gate-drain resistance is the reason behind the saturated state, which does not increase when applying further negative gate bias. Also, the gate threshold voltage is V_{th} = -3V, as identified from the plot of I_{DS}-V_{GS}, i.e., the normally-off (enhancement mode) is achieved.

The decrease in the maximum drain current in the positive surface charge model compared to that of the negative surface charge model corresponds to the shifted value of the threshold voltage to a negative value. Also, the main reason behind the decreasing drain current density of normally-off hydrogenated/diamond MOSFET is the high resistivity of the surface[15]. The improvement of field effect mobility is a requirement to confirm the high drain current density[24]. The threshold voltage value is controlled by the increased adsorption of the positive charge and the decreased adsorption of the negative charge. In addition, the main factor in achieving the normally-off state is the application of the deep donor doping in the substrate using nitrogen with $1x10^{16}$ cm^{-3} density. Fig. 5(b) shows the I_{DS}-V_{GS} characteristic, which reveals that the gate threshold voltage V_{th} leads to the fabrication of the device enhancement mode. In general, the threshold gate voltage V_{th} is described as the stable electrical voltage connected by the gate of the transistor for the control operation of the device. When the threshold voltage V_{th} gets a positive value, the channel becomes open, and the current will flow from drain to source. This phenomenon is called a normally-on (depletion mode). In contrast, when the threshold voltage is negative, the channel becomes close, then the current cannot flow well. This case is called normally-off or enhancement mode. In addition, the slope line which passes on the intersection between drain current I_{DS} and gate-source voltage V_{GS} constitutes the threshold gate voltage V_{th}. Also, applying a positive surface charge is required to increase the adsorption ion in the surface to gain a more negative value of threshold voltage, then achieving the enhancement mode (i.e., normally-off). On the other hand, the increased adsorption of positive charge and decreased adsorption of negative charge at surface shift the threshold voltage to a more negative value indicating the achievement of the enhancement mode [25].

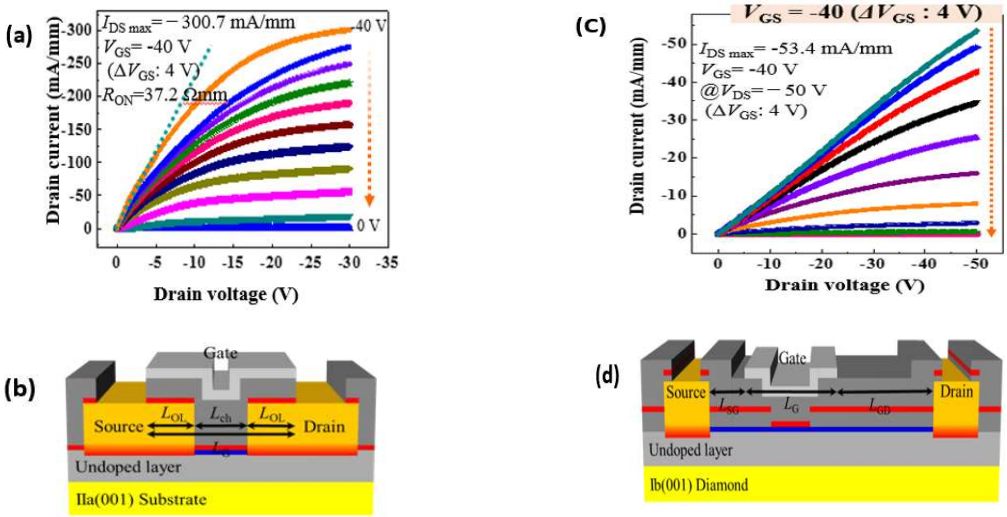

Figure 6. (a), (b) Schematic diagram of I_{DS}–V_{DS} characteristics of 2DHG Al_2O_3/diamond MOSFET after confirming the full SiO_2 layer close to the surface. Applied V_{DS} is in the range of -30V, and V_G -40V with a voltage step of 4V gives $I_{D\ MAX}$ -23.4 mA/mm. **(c), (d).** Schematic diagram of I_{DS}–V_{DS} characteristics of 2DHG Al_2O_3/diamond MOSFET after confirming partial SiO_2 layer under the gate. L_{SG}=2 µm, L_G=10 µm, L_{GD}=10 µm, W_G=25 µm, and the Si-Doped area=2 µm. $I_{D\ Max}$ = -53.4 mA/mm at V_{DS} -50 V, V_{GS} -40 V.

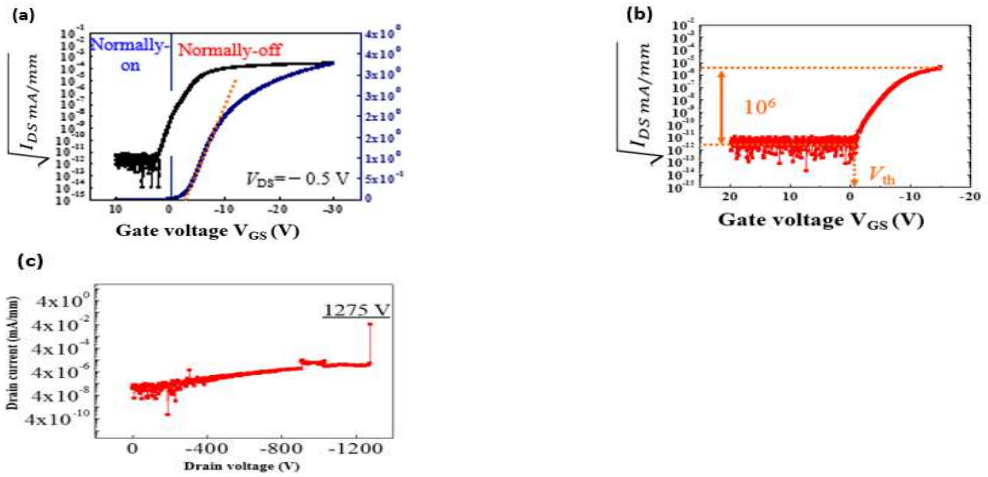

Figure 7. Schematic diagrams of I_{DS}-V_{GS} characteristics at drain voltage V_{DS} = -50 V. **(a)** Threshold voltage V_{th} = -2.7 V of the 2DHG full SiO_2/diamond MOSFET. **(b)** Threshold voltage V_{th} = -1.2 V of the 2DHG partial SiO_2/diamond MOSFET. Both indicat the normally-off state. **(c)** Schematic diagrams of 2DHG SiO_2/ diamond. The high breakdown voltage show with the device size L_{SD}=32 µm, L_{SG}=2 µm, L_G=10 µm, L_{GD}=20 µm, W_G = 25 µm, and the Si-Doped area = 2 µm.

To compare the simulation work with our experimental work[26], the fully and partially SiO_2 layers (4 nm) pinned under the gate, as gate insulator, in different C-H diamond/Al_2O_3 interfaces that confirmed the normally-off devices were achieved in various size devices. Fig. 6 (b) shows the MOSFET C-H structure with a full SiO_2 layer as the first device, in which the source gate distance is L_{SG} = 2 µm, the gate length is L_G = 4 µm and gate-drain distance is L_{GD} = 2 µm. The MOSFET device with a full SiO_2 layer exhibits the normally-off operation achieved at V_{th} = -2.7 V threshold voltage as shown in Fig. 7 (a) that is suitable for power device application. The threshold voltage is determined as the value that decreases the drain current by 6 orders from the maximum drain current. The maximum drain current density is $I_{D\ MAX}$ = -300.7 mA/mm at a drain voltage of V_{DS} =-35 V, and the gate voltage of V_{GS} = -40 V as illustrated in Fig 6 (a). Another MOSFET device with a partial SiO_2 layer located below the gate in C-H diamond/Al_2O_3 surface, in which L_{SG} = 2 µm, L_G = 10 µm, L_{GD} = 10 µm, W_G = 25 µm, and the Si-doped area = 2 µm, is depicted in Fig 6(c). Also, Fig. 6(d) shows the partial SiO_2 confirmed normally-off at the threshold voltage Vth = -1.2 V, as in Fig 7(b). Fig 6(c) shows that the maximum drain current density is $I_{D\ Max}$ = -53.4 mA/mm at V_{DS} = -50 V, and V_{GS} = -40 V[18]. The second MOSFET device uses a partial SiO_2 layer and the obtained experimental results correspond to the simulation work that confirmed normally-off operation using a positive surface charge model instead of SiO_2. Specifically, Fig 3(b) shows the 2DHG diamond MOSFET (normally-on) with transconductance characteristic g_m = 1.1mS/mm in the linear scale at drain voltage V_{DS} = -5V, and the hole mobility is 22.54 cm^2/Vs. We also simulated the positive surface charge MOSFET device (normally-off) with similar transconductance and hole mobility (drain voltage -5V with g_m=1.0 mS/mm) and μ =20.49 cm^2/Vs in Fig 5(b). Comparing with our experimental work, we determined that the 2DHG full SiO_2/diamond with transconductance and hole mobility were at a drain voltage of -5V, where g_m = 0.89 mS/mm and µ= 192.4 cm^2/Vs. We observed that the hole mobility for both the positive surface charge model and 2DHG SiO_2/diamond device was decreased when increasing the drain voltage. Also, the breakdown voltage was achieved in the MOSFET device with the SiO_2 layer at 1275V (Fig 7(c)). Overall, we fabricated 2DHG Al_2O_3/diamond MOSFETs and revealed that the normally-off operation can be obtained without deteriorating drain current density in both experiments and simulation works.

Conclusion

In this research article, we simulate and discuss the characteristics of the MOSFET device with deep doping using nitrogen in a low concentration obtained on 2DHG hydrogenated diamond using the 2D drift-diffusion model. As can be observed from the I-V characteristics of the device, the maximum drain current density is -52mA/mm, which is a complete pinch-off with a saturation region. However, this value is still lower than the current in the case of a negative and continuous surface charge model in the saturation region in which applying high gate voltage causes the highest gate-drain resistivity. The gate threshold voltage can be controlled and shifted to the negative value of V_{th}= -3 V when the applied positive surface charge is close to the interface, i.e., the normally-off state (enhancement mode) is achieved. The obtained simulated results correlate with the experimental work using the SiO_2 layer located below the gate in the C-H diamond with the Al_2O_3 surface. We then show how the surface band can be controlled when applying doping in the substrate under the effect of the surface charge. Also, the saturation behavior of the current in this model would be improved when the gate resistance is reduced using other related techniques, e.g., to add p+ type doping in the contact area. These promising results then bring new insight into this research theme and demonstrate that the proposal can facilitate various applications of p-channel diamond MOSFET devices, e.g., complementary power MOSFETs with trench gates as vertical FETs or the smart inverter systems with bulk conductions, to enable high breakdown voltage and low on-resistance, with less switching loss.

Methods

The device DC operation and gate threshold voltage V_{th} together with the I_{DS}-V_{DS} characteristics of the C-H diamond MOSFET are evaluated by simulation using Atlas TCAD as the two-dimensional (2D) device simulator software[27]. We used this software simulator to achieve both normally-off and normally-on characteristics by considering three typical C-H diamond MOSFET devices using various fixed surface charge models: negative surface charge, non-surface charge, and positive surface charge.

The device is under the thermal equilibrium conditions at 300^{o} K. Fig. 1 shows the C-H diamond MOSFET (1b 001) structure device modeling in an incomplete ionization model. The key parameters that are used for modeling devices include a diamond substrate (001) with a thickness of 500 nm and (Al) gate length (L_G) of 22 μm formed as the overlapping gate with a thickness of 100 nm. Also, Al_2O_3 is formed as Atomic Layer Deposition (ALD) with a thickness of 100 nm, channel length (L_{SD}) is 21μm, source and drain contacts are formed using Au/Ti. Other key diamond material parameters are summarized in Table 1 in which we show the real electron affinity of the diamond is -1.3 eV, but we considered it as zero due to the difficulty when applying a negative value in simulation (0 eV of EA). We also assumed the incomplete ionization of impurities model in the freeze-out region due to the default full-ionization of impurities (doping) in diamond, given that nitrogen shows an insulating behavior in the diamond. We then perform nitrogen and boron doping in diamond (500 nm) in a low concentration of $1x10^{16}$ cm^{-3} and $5x10^{15}$ cm^{-3}, respectively.

Parameters	Values of Diamond
Bandgap Eg	5.5 eV
Effective conduction band density of state (nc300)	$9.4x10^{18}$ cm^{-3}
Effective valence band density of state (nv300)	$1.4x10^{19}$ cm^{-3}
Effective Richardson constant of hole	100 A cm^{-2} K^{-2}
Hole mobility in the surface region (μp)	100 cm^2 / V.S

Carriers (hole) lifetime (TAUP0)	$1.0x10^{-9}$
Hole saturation velocity (VSATP)	$1x10^{7}$ cm/s
Electron affinity EA	0 (due to the feature of Hydrogenated diamond)

Table 1: Key parameters of the diamond material used for the modeling MOSFET device

We investigated the drift-diffusion model, which is the simplified form of the charge transport sheet model in Atlas. The mechanism used in this work is interface fixed charge, which defines the space charge using Poisson's equation with the ionized donor and acceptor. The mathematical model is established using the fundamental equations, including Poisson's equation and Maxwell's laws. Typically, the Poisson's equation is formed based on the electrostatic potential φ and space charge density ρ as depicted as the following equation:

$$\nabla(\varepsilon\nabla\varphi) = -\rho \quad (4)$$

In general, the space charge contains the mobile and fixed charges (electron, hole, and ionization energy of impurities). We assumed three space-charge models in this work, including the negative, positive, and neutral charge models of $-5x10^{12}$ cm^{-2}, and $5x10^{11}$ cm^{-2}, respectively. The continuity equation of electron and hole is given as:

$$\frac{\partial n}{\partial t} = \frac{1}{q}\nabla J_n + G_n - R_n \quad (5)$$

$$\frac{\partial p}{\partial t} = \frac{1}{q}\nabla J_p + G_p - R_p \quad (6)$$

where n is the electron concentration and p is the hole concentration, J_n and J_p are the electron and hole current densities, G_n and G_p are the electron and the hole generation rates. R_n and R_p are the recombination rates of electron and hole, respectively, and q is the magnitude of the charge on the electron. The carrier continuity equation in this model is then used for carrier density improvement as a result of transport, generation, and recombination processes for the specific hole, which only creates a wide bandgap of diamond and p-channel unipolar device by means of simulation.

References

1. Isberg, J. *et al*. High carrier mobility in single-crystal plasma-deposited diamond. *Science* **297**, 1670–1672 (2002).
2. Inaba, M. *et al*. Hydrogen-terminated diamond vertical-type metal oxide semiconductor field-effect transistors with a trench gate. *Appl. Phys. Lett.* **109**, 033503, (2016).
3. Kawarada, H., Hydrogen-terminated diamond surfaces and interfaces. *Surface Science Reports*. **26**, 205-259 (1996).
4. Kawarada, H. *et al.* Durability-enhanced two- dimensional hole gas of C-H diamond surface for complementary power inverter applications. *Scientific Reports* **7**, 42368 (2017).
5. Naramura, T. *et al*. Threshold voltage control of electrolyte solution gate field-effect transistor by electrochemical oxidation. *Appl. Phys. Lett.* **111**, 013505, (2017).
6. Hirama, K., Sato, H., Harada, Y., Yamamoto, H. & Kasu, M. Diamond field-effect transistors with 1.3 A/mm drain current density by Al_2O_{als} passivation layer. *Japanese Journal of Applied Physics* **51**, 090112 (2012).
7. Kawarada, H. High-Current Metal Oxide Semiconductor Field-Effect Transistors on H-Terminated Diamond Surfaces and Their High-Frequency Operation. *Jpn. J. Appl. Phys* **51,** 090111 (2012).
8. Kawarada, H., Hydrogen-terminated diamond surface a d interface. *Surface Science Reports* **26**, 205-259 (1996).
9. Harris, S.J., Goodwin, D.G. Growth on the reconstructed diamond (100) surface. *Journal of Physical Chemistry*, **97**, pp.23-28 (1993).
10. Cui, J. B., Ristein, J., Ley, L., Electron Affinity of the Bare and Hydrogen Covered Single Crystal Diamond (111) Surface. *Phys. Rev. Lett*. **81**, 429 (1998).
11. Maier, F., Ristein, J., Ley, L., Electron affinity of plasma-hydrogenated and chemically oxidized diamond (100) surfaces. *Phys. Rev. B* **64**,165411 (2001).
12. Tsugawa, K. *et al*. High-performance diamond surface-channel field-effect transistors and their operation mechanism. *Diam. Relat. Mater*. **8**, 927-933 (1999).

13. Reem, A., Mohammed, A., Quang, N., N., Kawarada, H., Characterization and Analysis of Two-dimensional Hydrogenated Nanocrystalline-diamond Metal Oxide Semiconductor Field Effect Transistor (MOSFET) using Different Surface Charge Models with Device Simulation. *2020 IEEE 20th International Conference on Nanotechnology* (IEEE-NANO, 2020).
14. Kitabayashi, Y. *et al*. Normally-off C-H diamond MOSFETs with partial C-O channel achieving 2-kv breakdown voltage. *IEEE Electron Device Letters* **38**, 3 (2017).
15. Nobutaka, O. *et al*. Normally-off two-dimensional hole gas diamond MOSFETs through nitrogen-ion implantation. *IEEE Elec. Dev. Lett*. **40**, 6, (2019).
16. Saito, W., Takada, Y., Kuraguchi, M., Tsuda, K., Omura, I. Recessed-gate structure approach toward normally off high-Voltage AlGaN/GaN HEMT for power electronics applications. *IEEE Transactions on Electron Devices* **53**, 2 (2006).
17. Liu, J., Koide, Y. *et al.,* Electrical characteristics of hydrogen terminated diamond metal-oxide semiconductor with atomic layer deposited HfO2 as gate dielectric. *Appl. Phys. Lett*. **102**, 112910 (2013).
18. Wenxi Fei, Te Bi, Iwataki, M., Imanishi, S., Kawarada, H., Oxidized Si terminated diamond and its MOSFET operation with SiO2 gate insulator. *Appl. Phys. Lett.* 116, 212103 (2020).
19. Collins, A.T. The fermi level in diamond. *Journal of Physics: Condensed Matter* **14**, 3743-3750 (2002).
20. Jin, S., Moustakas, T. D., Effect of nitrogen on the growth of diamond films, *applied physics letters*, **65**,403 (1994).
21. Kalish, R., The search for donors in diamond. *Diamond and Related Materials* **10**, 1749-1755 (2001).
22. Bhattacharyya*, S., et al.* Synthesis and characterization of highly conducting nitrogen-doped ultrananocrystalline diamond films. *Appl. Phys. Lett*. **79**, 1441 (2001).
23. Tsugawa, K., Umezawa, H., Kawarada, H., Characterization of diamond surface-channel metal-semiconductor field-effect transistor with device simulation. *Japanese Journal of Applied Physics.* **40**, 5A (2001).
24. Matsumoto. T. *et al*., Inversion channel diamond metal-oxide-semiconductor with normally off characteristics. *scientific reports.* **6**, 31585 (2016).
25. Kawarada, H., Ruslinda, A.R. Diamond electrolyte solution gate FETs for DNA and protein sensors using DNA/RNA aptamers. *Physica Status Solidi A*. **208**,2005-2016 (2011).
26. Yabe, T. *et al*. Normally off 2DHG Al2O3/SiO2 MOSFETs without deteriorating drain current density. *International conference of Material Research Socity Fall Meeting* (MRS, 2018).
27. Patrick. H. D. *Atlas user's manual device simulation software* https://silvaco.com/ (2016).

Acknowledgments

This research was supported in part by the Institute of Nanoscience and Nanotechnology from Waseda University, Japan, for the use of their equipment. Q.N.N.'s work was funded by Waseda University Grant for Special Research Projects. The authors would like to extend our gratitude to Alhasani Mohammed and Malak Jalal for their help use and perform Atlas TCAD simulation.

Author Contributions

H.K. conceived the idea. R.A. fabricated and performed FETs device simulation and measured their characteristics. Also, R.A. wrote the initial draft of the manuscript. T.Y. fabricated the 2DHG diamond Al_2O_3/SiO2 MOSFETs and measured device operation and the I-V characteristics. Y.I, N.O., and S.I. performed the calculated task. Q.N.N. reviewed and edited the manuscript with the help of all co-authors.

Additional Information

Competing interests: The authors declare no competing interests.

Publisher's note: Springer Nature remains neutral with regard to jurisdictional claims in published maps and institutional affiliations.

Figures

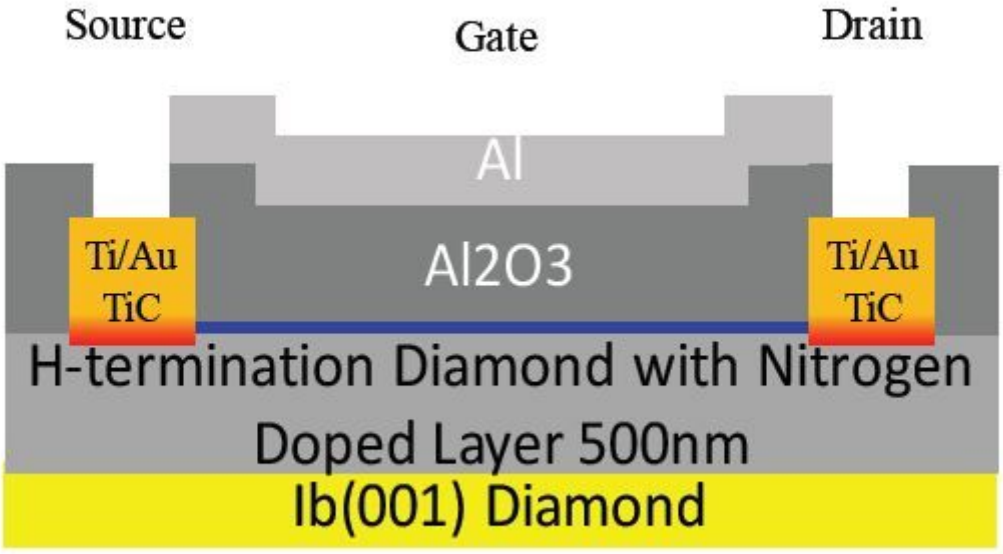

Figure 1

Cross-sectional representation of the 2DHG diamond MOSFET with deep donor nitrogen doping (500 nm) where LG = 22 μm, Lch =21 μm and WG = 25 μm.

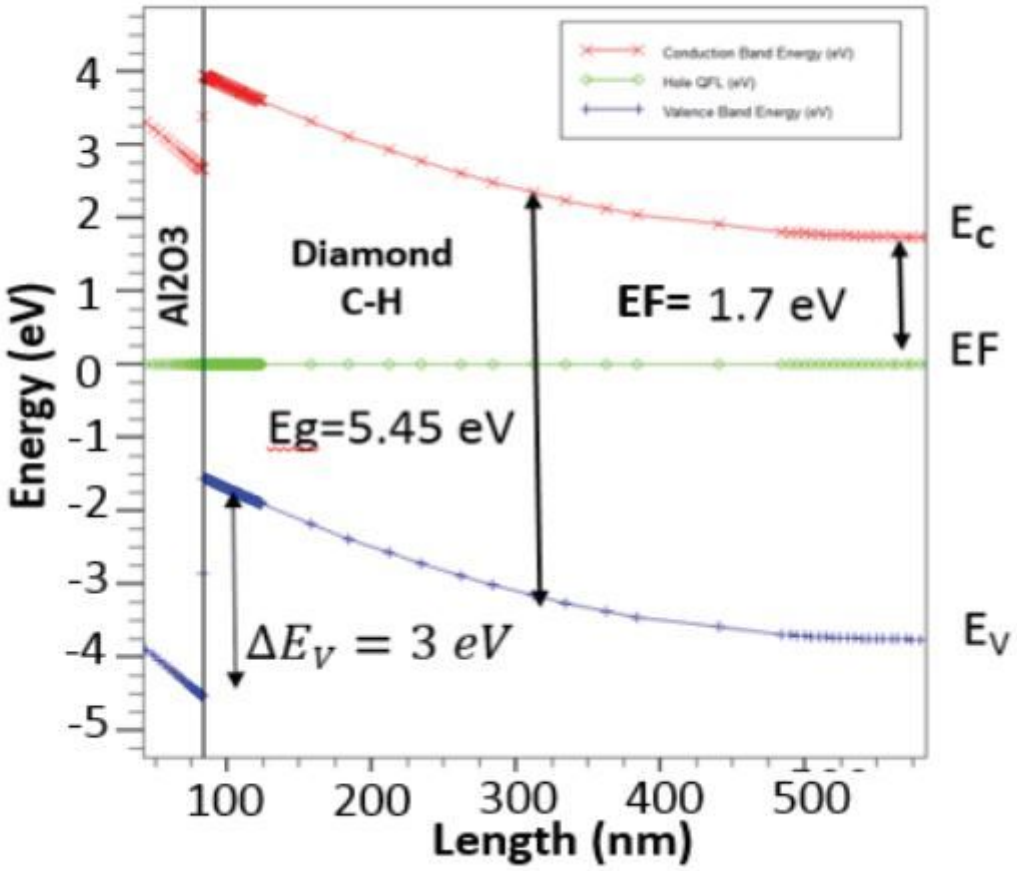

Figure 2

Schematic energy diagrams of the 2DHG diamond MOSFET device. The band of hydrogynated diamond become upward in the positive surface charge model with N deep doping (1.7 eV) at the inversion layer.

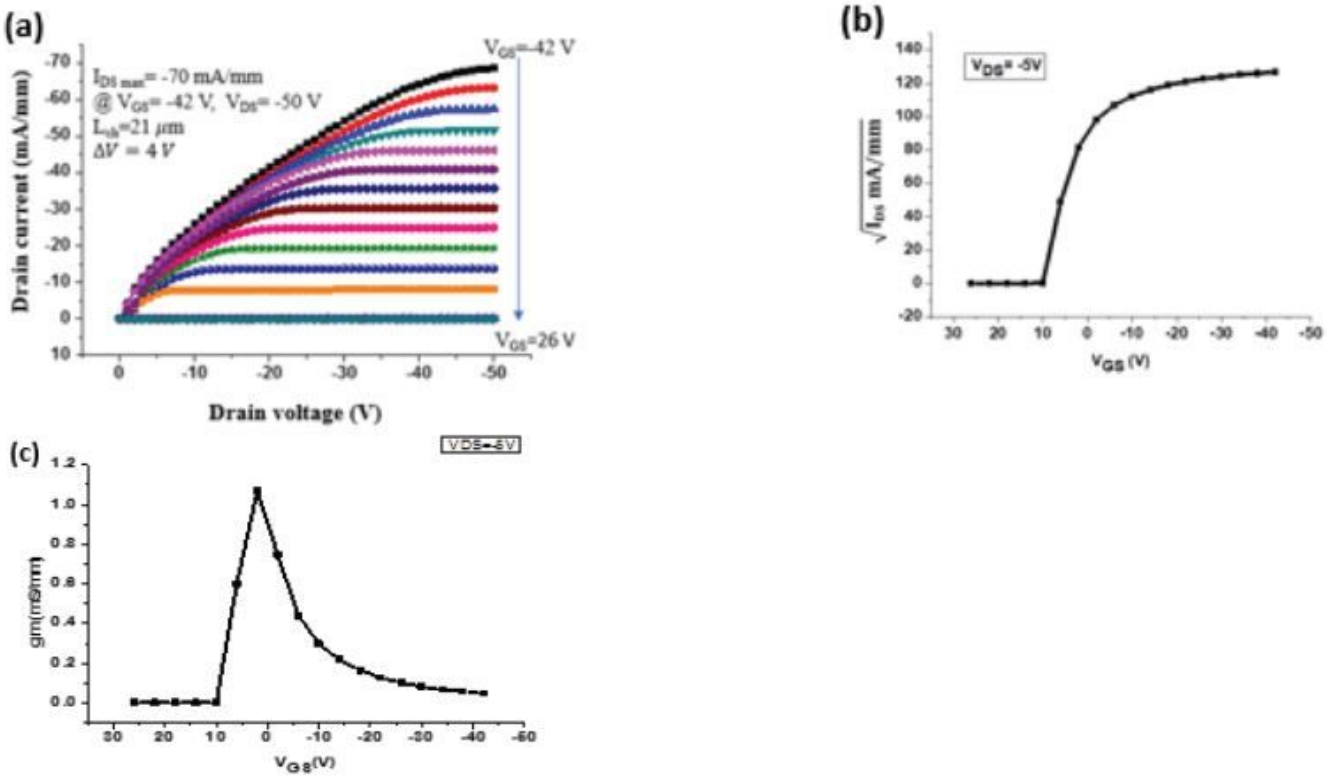

Figure 3

Schematic diagram of characteristics of 2DHG diamond MOSFET in a negative surface charge model. Applied Qf= -5x1012 cm-2 with N doping layer. (a) The IDS Max= -70 mA/mm at VDS is in the range of 50 V, and VG ranges from 26V to -42 V with a voltage step of 4 V. (b) Threshold voltage Vth = 10 V indicating the normally-on state at VDS = -5 V. (c) Transconductance of device gm=1.1 mS/mm.

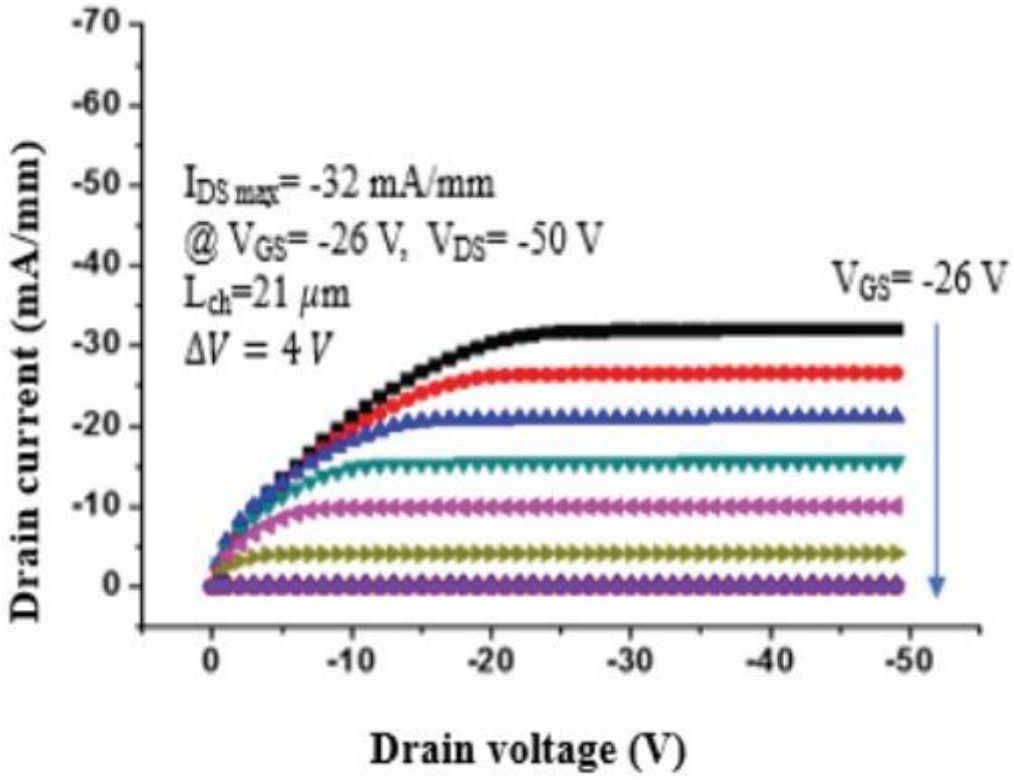

Figure 4

Schematic diagram of IDS–VDS characteristics of 2DHG diamond MOSFET in the natural surface charge model (non-charged) with N doping layer. Applied VDS is in the range of 50V, and VG ranges from 26 V to -26 V with a voltage step of 4 V.

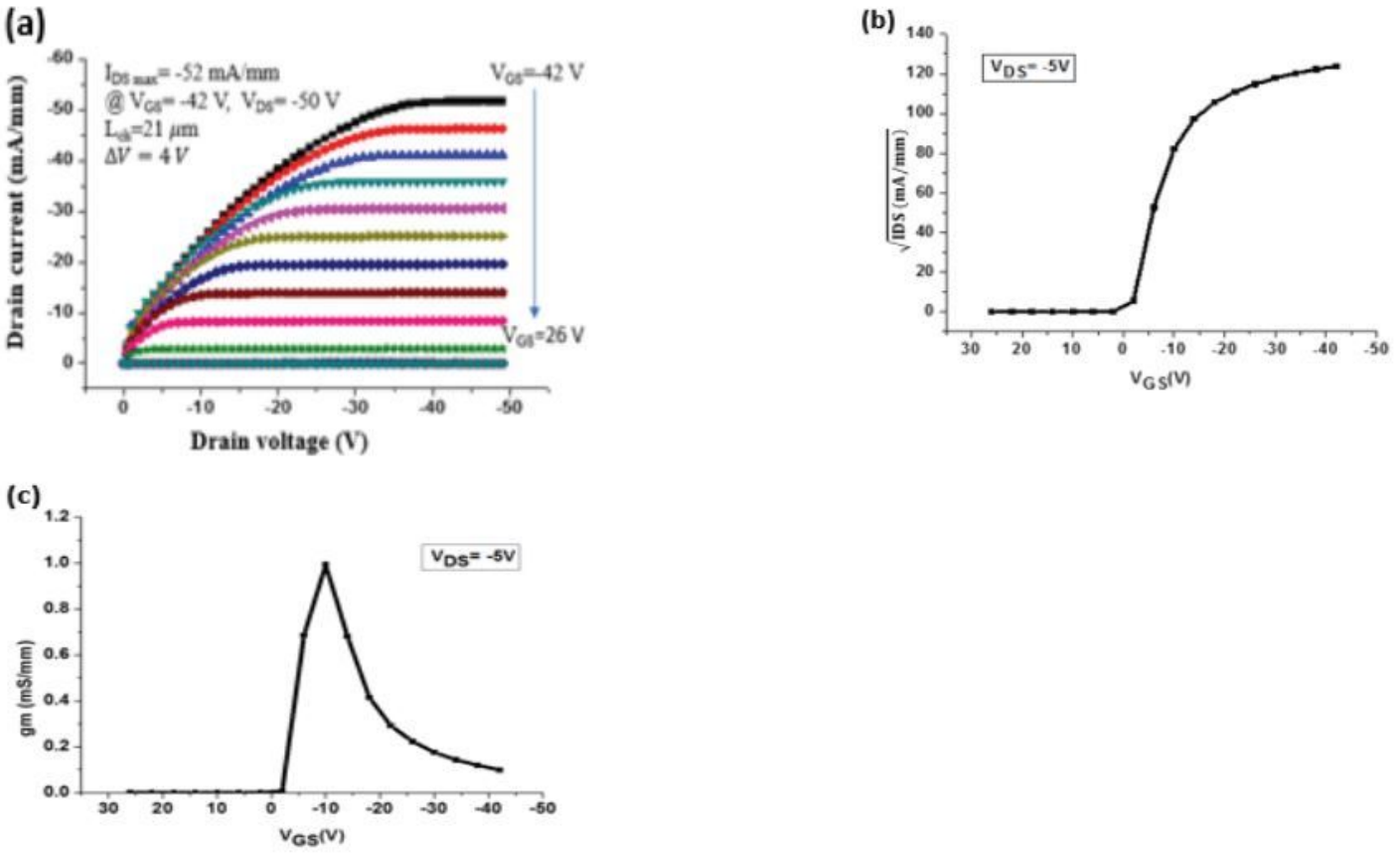

Figure 5

Schematic diagram of output characteristics of 2DHG diamond MOSFET positive surface charge model of 5x1011cm-2 with nitrogen doping layer in concentration at 1x1016cm-3 at room temperature. (a) IDS-VDS characteristics, the IDS Max= -52 mA/mm at VDS is in the range of 50 V, and VG ranges from 26V to -42 V with a voltage step of 4 V (b) Threshold voltage Vth = -3V at drain voltage VDS = -5 V indicating the normally-off state. (c) Transconductance of device gm = 1.0 mS/mm.

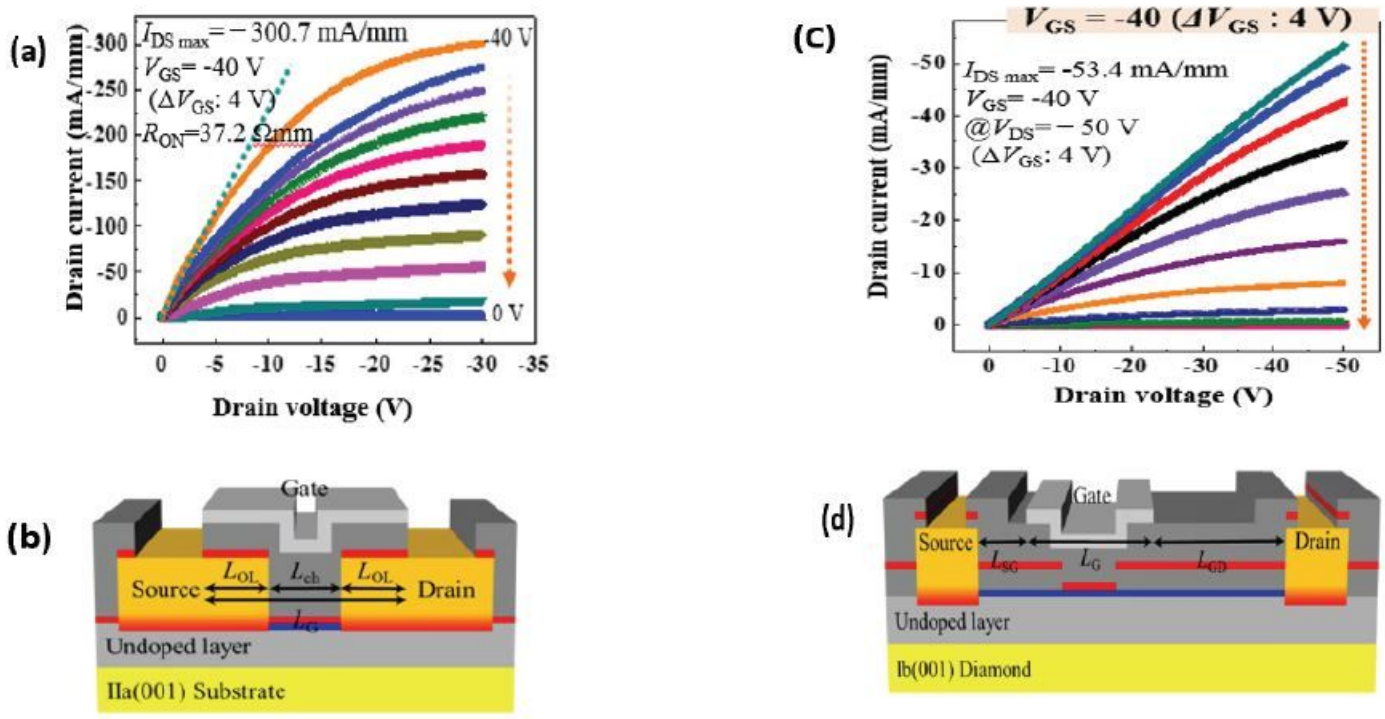

Figure 6

(a), (b) Schematic diagram of IDS–VDS characteristics of 2DHG Al2O3/diamond MOSFET after confirming the full SiO2 layer close to the surface. Applied VDS is in the range of -30V, and VG -40V with a voltage step of 4V gives ID MAX -23.4 mA/mm. (c), (d). Schematic diagram of IDS–VDS characteristics of 2DHG Al2O3/diamond MOSFET after confirming partial SiO2 layer under the gate. LSG=2 µm, LG=10 µm, LGD=10 µm, WG=25 µm, and the Si-Doped area=2 µm. ID Max = -53.4 mA/mm at VDS -50 V, VGS -40 V.

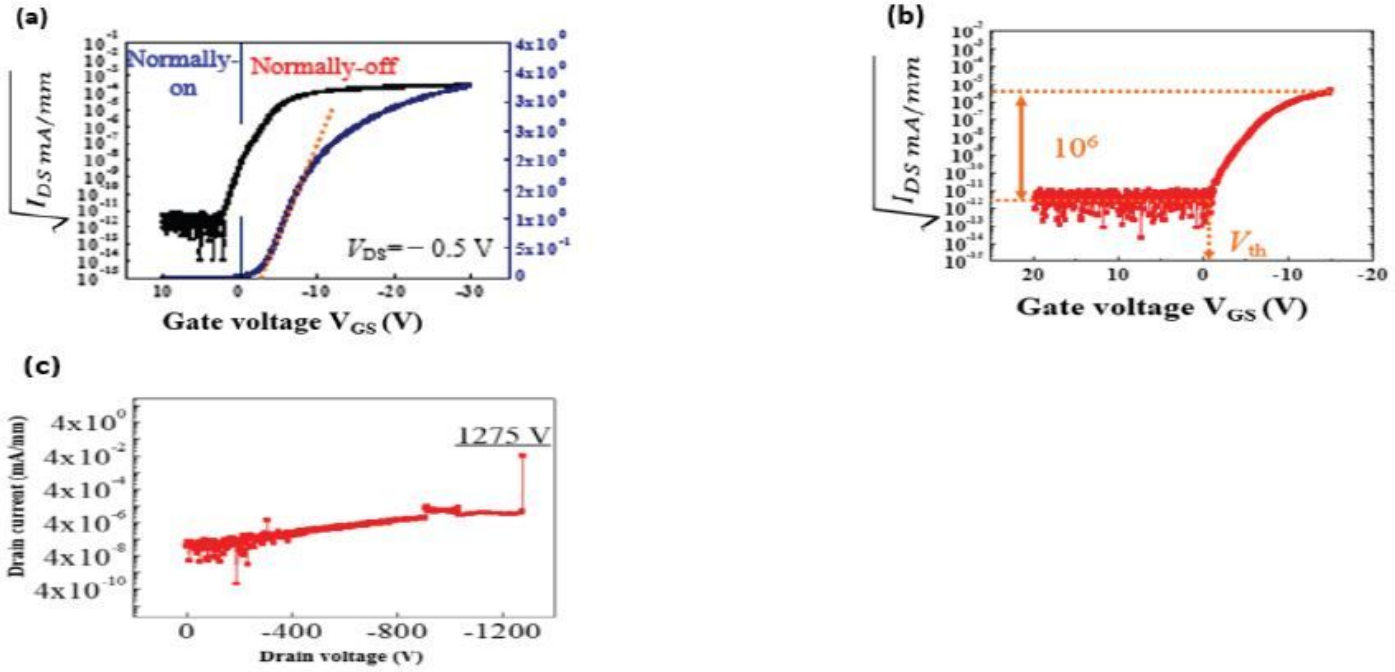

Figure 7

Schematic diagrams of IDS-VGS characteristics at drain voltage VDS = -50 V. (a) Threshold voltage Vth = -2.7 V of the 2DHG full SiO2/diamond MOSFET. (b) Threshold voltage Vth = -1.2 V of the 2DHG partial SiO2/diamond MOSFET. Both indicat the normally-off state. (c) Schematic diagrams of 2DHG SiO2/diamond. The high breakdown voltage show with the device size □SD=32 μm, □SG=2 μm, □G=10 μm, □□□=20 μm, WG = 25 μm, and the Si-Doped area = 2 μm.